Transient Bloch oscillation with the symmetry-governed phase in semiconductor superlattices

T. Unuma,[1,2,*] Y. Ino,[3] M. Kuwata-Gonokami,[3] G. Bastard,[4] and K. Hirakawa[1,†]
[1]*Institute of Industrial Science and INQIE, University of Tokyo, 4-6-1 Komaba, Meguro-ku, Tokyo 153-8505, Japan*
[2]*Department of Applied Physics, Nagoya University, Furo-cho, Chikusa-ku, Nagoya 464-8603, Japan*
[3]*Department of Applied Physics and INQIE, University of Tokyo, 7-3-1 Hongo, Bunkyo-ku, Tokyo 113-8656, Japan*
[4]*Laboratoire Pierre Aigrain, Ecole Normale Supérieure, 24 rue Lhomond, F75005 Paris, France*
(Received 7 November 2009; revised manuscript received 16 February 2010; published 25 March 2010)

We have investigated the time evolution of electron transport in the lowest miniband of semiconductor superlattices for various initial electron distributions created by femtosecond laser pulses. It is found that the terahertz wave forms emitted by the transient motion of Bloch oscillating electrons are insensitive to the pump photon energy and that the current starts from its maximum as damped cos $\omega_B t$ (ω_B: Bloch frequency), in contrast to the expectation from semiclassical miniband transport. We show that the translationally symmetric electron distribution on the Wannier-Stark ladder is essential for the observed unique oscillation phase.

DOI: 10.1103/PhysRevB.81.125329 PACS number(s): 78.47.−p, 73.21.Cd, 73.50.Mx, 78.67.Pt

I. INTRODUCTION

Charge transport in biased crystals is one of the most fundamental subjects in solid-state physics. A peculiar aspect of this was noticed by Bloch[1] and Zener[2] around 1930: a repetition of Bragg reflections in the semiclassical energy-momentum dispersion relation, as currently called the Bloch oscillation. In quantum mechanics, the Bloch oscillation is described as the formation of equidistant energy levels, namely, the Wannier-Stark (WS) ladder.[3] As schematically illustrated in Fig. 1, these two pictures are related to each other in such a way that the energy separation between any two neighboring levels in the WS ladder is equal to the product of the Planck constant and the Bloch frequency for the semiclassical acceleration in the Brillouin zone. Here, the Bloch frequency is given by $\omega_B = eFd/\hbar$ with F being the dc bias electric field and d being the lattice constant. The Bloch oscillation has never been observed in bulk solids because electron scattering rates are much higher than ω_B for their subnanometer lattice constants. Since Esaki and Tsu[4] proposed in 1970 an idea of miniaturizing the Brillouin zone, semiconductor superlattices (SLs) have been an ideal system for investigating electronic properties in single energy bands, and intriguing properties related to Bloch oscillations in both steady states[5–8] and transient transport[9–12] have been reported.

So far, it has been commonly believed that the semiclassical band picture and the WS ladder picture can be equivalently used, depending on whichever is more convenient, to describe various kinds of transport phenomena in semiconductor SLs.[13,14] However, the equivalence between the two pictures has never been critically examined; it has been verified only for a few properties in steady states,[15,16] where Bloch oscillations are dephased.

In this work, we have demonstrated that the equivalence between the two pictures breaks down for the transient transport of Bloch oscillating electrons. Our phase-sensitive measurement of terahertz (THz) electric fields emitted from GaAs-based SLs reveals that the transient current always starts from its maximum as damped cos $\omega_B t$ for various initial electron distributions created by femtosecond laser pulses. We show that the observed oscillation phase cannot be explained from semiclassical electron distributions in momentum space and is governed by the translationally symmetric electron distribution under WS localization of electron wave functions.

II. EXPERIMENT

The sample used in this study was an undoped GaAs(7.5 nm)/AlAs(0.5 nm) SL grown by molecular-beam epitaxy on a (001) n^+-GaAs substrate. The miniband structure of this SL potential was calculated using the Kronig-Penney model: the ground miniband is 45 meV wide and separated from the first excited miniband by a 93-meV-wide minigap.[17] To apply dc bias electric fields to the sample, we fabricated a semitransparent NiCr Schottky contact on the front surface and a Au-GeNi Ohmic contact on the back surface. Electrons were created in the ground miniband by light pulses with a temporal width of ~100 fs delivered from a tunable mode-locked Ti:sapphire laser. Since no sign of Zener tunneling

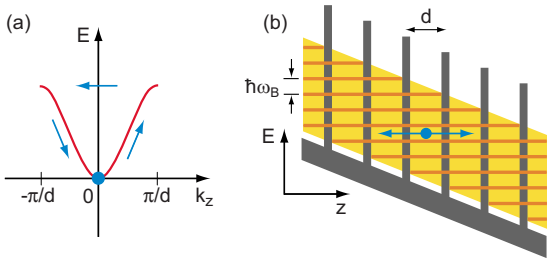

FIG. 1. (Color online) Two physical pictures predicting Bloch oscillations in biased crystals with lattice constant d along the z axis. (a) Semiclassical band picture: under dc bias electric fields F, electrons in a single energy band (solid curve drawn in momentum space) are accelerated and experience Bragg reflections from $k_z = \pi/d$ to $-\pi/d$ repeatedly at the Bloch frequency $\omega_B = eFd/\hbar$. (b) Wannier-Stark ladder picture: in quantum mechanics, the energy band (parallelogram region drawn in real space) is split into discrete levels (horizontal bars) with equal energy separation by $\hbar\omega_B$. Electrons exhibit quantum beats at the Bloch frequency ω_B before reaching the steady states.

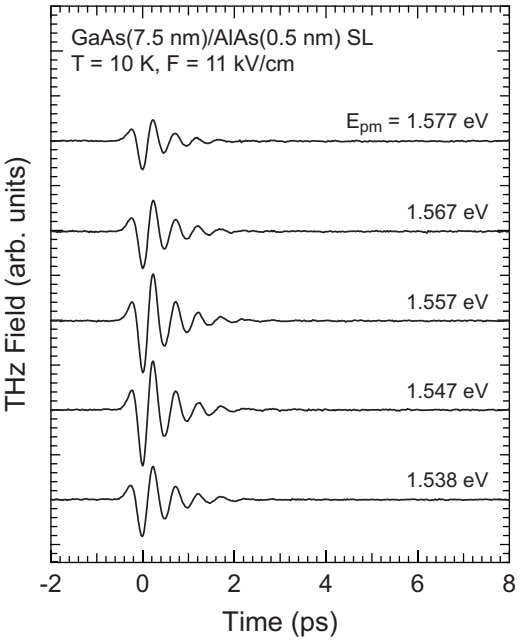

FIG. 2. Temporal wave forms of the THz electric fields emitted from a GaAs(7.5 nm)/AlAs(0.5 nm) SL at $F=11$ kV/cm for various pump photon energies E_{pm}. The time origin ($t=0$) shown here is arbitrary. The values of 1.538 and 1.577 eV for E_{pm} correspond to the photoexcitation of electrons near the bottom and the top of the ground miniband, respectively.

into higher minibands was observed, electron transport took place only in the ground miniband in the electric field range studied here. For various central photon energies of the pump light pulses E_{pm}, transient THz electric fields emitted from the sample were recorded in the time domain using a 0.1-mm-thick (110) ZnTe electro-optic sensor, which has a flat sensitivity up to 3.5 THz. The THz signals are dominated by electron motion, because the miniband for heavy holes is much narrower than that for electrons and the optical absorption for light holes is only 1/3 of that for heavy holes.[18,19] In the experiment, the dc photocurrent was kept constant with the electron concentration as low as $\sim 1\times 10^{14}$ cm^{-3} to avoid the field-screening effect. All the measurements were performed at 10 K.

III. RESULTS AND ANALYSIS

Figure 2 shows the temporal wave forms of the THz electric fields emitted from the sample at $F=11$ kV/cm for $E_{pm}=1.538-1.577$ eV, with a time origin placed at a tentative position. The values of 1.538 and 1.577 eV for E_{pm} correspond to the photoexcitation of electrons near the bottom and the top of the ground miniband, respectively. For $E_{pm}<1.538$ eV, neither THz emission nor dc photocurrent was observed because E_{pm} is too low for interband photoexcitation. As seen in the figure, the THz wave forms have a characteristic feature consisting of an initial small positive peak at −0.23 ps and a subsequent damped sinusoidal oscillation. This oscillatory part has a frequency of 2.0 THz and is, indeed, nearly equal to the expected Bloch frequency eFd/h.[19] It should be noted that the observed THz wave forms are very insensitive to the change in E_{pm}. This behavior is surprising in the framework of semiclassical miniband transport because, when E_{pm} is varied, different initial electron distributions should be created in the mini-Brillouin zone.

To clarify how the transient electron transport starts and evolves in biased SLs, we first determined the time origin of the THz wave forms accurately, i.e., we removed a misplacement δt of the time origin by applying an elaborate algorithm, the maximum-entropy method (MEM), to the THz wave forms $E_{THz}(t)$ of Fig. 2. The principle of the MEM for THz emission spectroscopy is very similar to that for THz reflection spectroscopy.[20] The MEM extracts resonance features from the power spectrum $|\tilde{E}_{THz}(\omega)|^2$ of measured THz wave forms and calculates phase shifts $\psi_M(\omega)$ across the resonances. Here, the tilde denotes the Fourier transform and $\psi_M(\omega)$ is called the MEM phase. The remaining part in the phase spectrum, $\varphi_{err}(\omega)=\arg \tilde{E}_{THz}(\omega)-\psi_M(\omega)$, is called the error phase and originates from small random noise and a systematic shift by $-\omega\delta t$ due to misplacement of the time origin. It should be noted that, since $|\tilde{E}_{THz}(\omega)|^2$ does not depend on the position of $t=0$, the misplacement of the time origin does not affect $\psi_M(\omega)$ and appears only in $\varphi_{err}(\omega)$. The separation between $\psi_M(\omega)$ and $-\omega\delta t$ is a great advantage in determining δt, which has never been achieved by empirical methods.[19,21,22]

Numerical analysis of $E_{THz}(t)$ by the MEM is shown in Fig. 3 for the data taken at $E_{pm}=1.538$ eV of Fig. 2, where electrons are supposed to be created near the bottom of the ground miniband. Figure 3(a) shows the amplitude spectrum $|\tilde{E}_{THz}(\omega)|$ and the phase spectrum $\arg \tilde{E}_{THz}(\omega)$ computed from the measured THz wave form with the tentative time

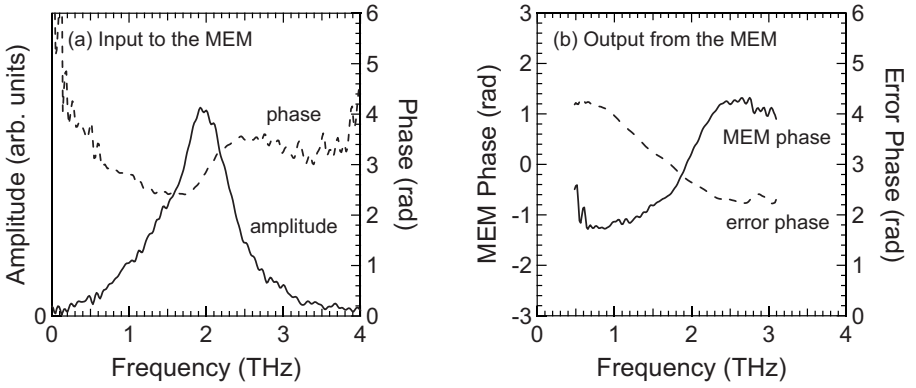

FIG. 3. MEM analysis of the THz emission data taken at $E_{pm}=1.538$ eV. (a) Fourier spectrum (amplitude and phase) computed from the THz wave form with the tentative time origin of Fig. 2. (b) Output spectral data for the MEM phase and error phase.

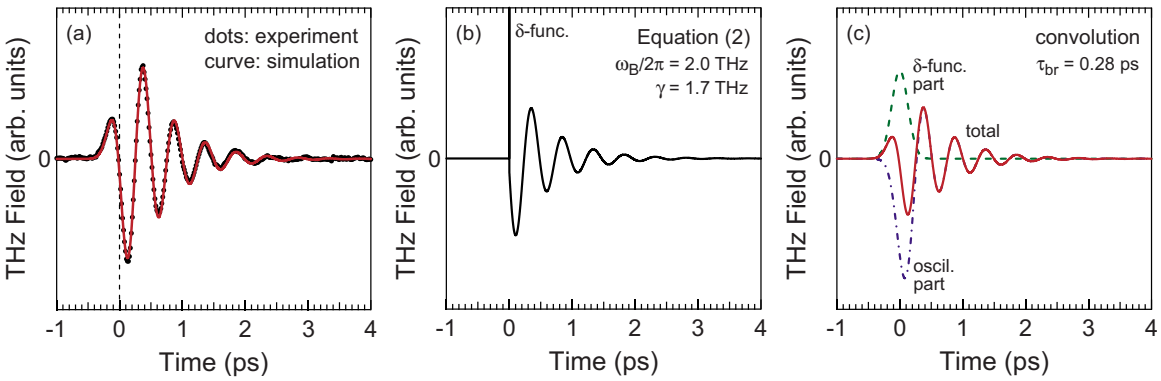

FIG. 4. (Color online) (a) Observed THz wave form plotted by dots with the corrected position of $t=0$ (vertical dashed line). Also shown by a solid curve is a simulated THz trace expected for a damped cos $\omega_B t$ current convolved with a temporal broadening of $\tau_{\rm br}=0.28$ ps. Details of the simulated THz trace: (b) $\partial J_p(t)/\partial t$ given by Eq. (2) with fitting parameters $\omega_B/2\pi=2.0$ THz and $\gamma=1.7$ THz. (c) Convolutions for the delta-function part (dashed curve), damped-oscillation part (dash-dotted curve), and total (solid curve) of $\partial J_p(t)/\partial t$.

origin of Fig. 2. We then feed the obtained $|\tilde{E}_{\rm THz}(\omega)|$ and $\arg \tilde{E}_{\rm THz}(\omega)$ into the MEM analysis. Figure 3(b) shows the output from the MEM, i.e., the MEM phase spectrum $\psi_M(\omega)$ and the error-phase spectrum $\varphi_{\rm err}(\omega)$. As seen in the figure, the MEM phase $\psi_M(\omega)$ displays a phase shift by π across the resonance feature in $|\tilde{E}_{\rm THz}(\omega)|$, while the error phase $\varphi_{\rm err}(\omega)$ exhibits a linear change for $\omega/2\pi=1.0$–2.5 THz, which arises from the misplacement of the time origin. By compensating for the slope of $\varphi_{\rm err}(\omega)$, we estimated δt to be 150 ± 15 fs for the original input data shown in Fig. 2.

The THz wave form after the removal of δt is plotted in Fig. 4(a) by dots. The vertical dashed line in the figure denotes the corrected position of $t=0$, indicating that the oscillatory THz signal for $t>0$ evolves nearly as damped $-\sin \omega_B t$ and that the small positive signal for $t<0$ is not part of the damped sinusoidal oscillation.

Since the emitted THz electric field is proportional to the time derivative of current, we examined how well the observed THz wave form can be reproduced by a simulated damped sinusoidal oscillation current of the form

$$J_p(t) = J_1 \Theta(t) e^{-\gamma t} \cos \omega_B t, \tag{1}$$

where J_1 is the maximum value of the current, $\Theta(t)$ the unit step function, and γ the dephasing rate. The physical meaning of Eq. (1) will be seen later. Differentiation of Eq. (1) leads to

$$\frac{\partial J_p}{\partial t} = J_1[\delta(t) - \Theta(t)e^{-\gamma t}(\omega_B \sin \omega_B t + \gamma \cos \omega_B t)], \tag{2}$$

where $\delta(t)$ is the delta function. Equation (2) was compared with the observed THz wave form after it was convolved with a temporal broadening function characterized by $\tau_{\rm br}$ (=0.28 ps) due to the finite bandwidth of our experimental setup.

The simulated trace of $\partial J_p(t)/\partial t$ given by Eq. (2) with fitting parameters $\omega_B/2\pi=2.0$ THz and $\gamma=1.7$ THz (Ref. 23) is shown in Fig. 4(b). Also plotted in Fig. 4(c) are the delta-function part (dashed curve), the damped-oscillation part (dash-dotted curve), and the total (solid curve) of $\partial J_p(t)/\partial t$ convolved with the temporal broadening function. The total simulated THz trace is replotted into Fig. 4(a) by a solid curve. As seen in the figure, the agreement between the observed THz wave form and the simulated THz trace is excellent. This indicates that the transient current indeed starts from its maximum as damped cos $\omega_B t$ [see Eq. (1)] in biased SLs. When we look at Fig. 4(c) more closely, we further notice that the initial small positive signal for $t<0$ of Fig. 4(a) is reminiscent of the delta function in $\partial J_p(t)/\partial t$ at $t=0$. It should be noted that such a transient current expressed by Eq. (1) has never been predicted by existing theories. Particularly, in the semiclassical band picture, Eq. (1) requires assuming an unrealistic electron distribution around the middle of the miniband at $t=0$ even for the lowest value of $E_{\rm pm}$.

The same analysis works for the THz emission data taken at different dc bias electric fields F. Figure 5 shows the observed THz wave forms (dots) at $E_{\rm pm}=1.547$ eV for $F=8.9$, 11, and 13 kV/cm plotted with the corrected position of t

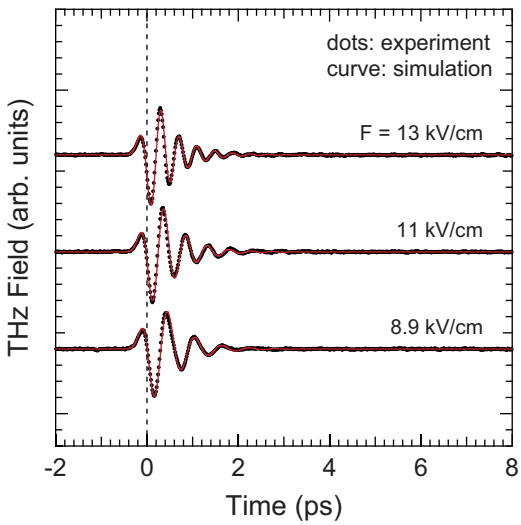

FIG. 5. (Color online) Observed THz wave forms for various dc bias electric fields $F=8.9$, 11, and 13 kV/cm plotted by dots with the corrected position of $t=0$ (vertical dashed line). Also shown by solid curves are simulated THz traces expected for a damped cos $\omega_B t$ current with $\omega_B/2\pi=1.7$, 2.1, and 2.5 THz, respectively.

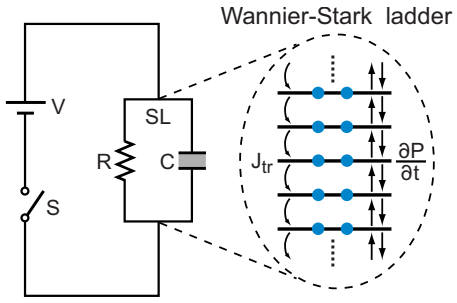

FIG. 6. (Color online) Equivalent circuit for the WS ladder system. C: dielectric-inserted capacitor, R: resistor, V: voltage source, and S: optical switch. Here, electrons are equally distributed onto all the WS levels. Each electron contributes either to the polarization current $\partial P(t)/\partial t$ through C (due to the quantum beat) or to the true current J_{tr} through R (due to the hopping transport) with a probability governed by inter-WS-level scattering.

=0 (vertical dashed line). They can be well reproduced by simulated THz traces (solid curves) when the fitting parameter $\omega_B/2\pi$ of Eq. (2) is varied from 1.7 to 2.5 THz, nearly satisfying the relation $\omega_B=eFd/\hbar$. This provides further support for the analysis described above.

IV. DISCUSSION

Below, we discuss the mechanism for the observed transient current by considering WS localization of electron wave functions under dc bias electric fields. In the WS ladder picture, since electrons are bound to the WS levels and occasionally undergo inter-WS-level scattering, both the quantum beat of polarization charges and the hopping transport of true charges start at the moment of short-pulse photoexcitation. Here, due to the translational symmetry of lattice structures, all the WS levels are equally populated by electrons for $t>0$.[24] This unique electron distribution in real space allows us to intuitively understand the observed E_{pm}-insensitive oscillation phase by treating the WS ladder as *a leaky dielectric medium composed of quantum-well artificial mesoscopic molecules* in a biased SL.

On the basis of this insight, we propose an equivalent circuit for the WS ladder system. The circuit diagram is shown in Fig. 6, which consists of a dielectric-inserted capacitor C for polarization charges, a resistor R for true charge transport, a voltage source V for the bias electric field F, and a switch S for short-pulse photoexcitation that triggers electron motion. Here, the formation of a WS ladder is reflected in the resistor R via the inter-WS-level scattering time and in the capacitor C via the dielectric susceptibility $\chi(\omega)$ that has a resonance at $\omega\simeq\pm\omega_B$. Electrons distributed onto the WS ladder leads to

$$\mathrm{Im}\ \chi(\pm\omega_B)=0, \tag{3}$$

i.e., a perfect cancellation of the absorption and stimulated emission at the Bloch frequency.[24]

When the optical switch S is suddenly closed at $t=0$, electrons are subjected to a step-function-like electric field $F(t)=F\Theta(t)$. The total current for $t>0$ is expressed as

$$J_{\mathrm{tot}}(t)=\frac{\partial P(t)}{\partial t}+J_{\mathrm{tr}}, \tag{4}$$

where $\partial P(t)/\partial t$ is the polarization current through capacitor C (coherent transient motion due to the quantum beat), and J_{tr} is the true current through resistor R (incoherent steady motion due to the hopping transport, which gives rise to the Esaki-Tsu dc conductivity).[25] Since the polarization increases linearly with the bias electric field in the WS ladder regime, it is given by $\tilde{P}(\omega)=\chi(\omega)\tilde{F}(\omega)$ with $\tilde{F}(\omega)=F/(a-i\omega)$ in the limit of $a\rightarrow+0$. Thus, for $t>0$, we obtain a crude expression for $\partial P(t)/\partial t$ by picking up the $e^{\pm i\omega_B t}$ components with a damping factor $e^{-\gamma t}$:

$$\frac{\partial P}{\partial t}=\frac{F}{2\pi}\int_{-\infty}^{\infty}d\omega\chi(\omega)e^{-i\omega t} \tag{5}$$

$$\sim\gamma\,\mathrm{Re}\ \chi(\omega_B)Fe^{-\gamma t}\cos\omega_B t, \tag{6}$$

which indeed agrees with the trial expression for $J_p(t)$ given by Eq. (1). A physical interpretation of Eq. (6) is that, since the step-function-like input electric field $F(t)$ is antisymmetric with respect to $t=0$ and includes a sin $\omega_B t$-like driving field, the polarization current $\partial P(t)/\partial t$ must be orthogonal to it and have the form of cos $\omega_B t$ to produce a dissipationless current at the Bloch frequency.

Now, let us discuss the reason why the semiclassical band picture does not work correctly for the observed oscillation phase. In the semiclassical band picture, electrons would be accelerated (e.g., from the bottom of the miniband for the lowest-energy photoexcitation) as if they were spatially extended in the initial half cycle of the Bloch oscillation; they would not "feel" the spatial localization until they experience Bragg reflections many times. Therefore, the semiclassical band picture cannot give a good description for physical situations where electrons are suddenly created in the states that are already spatially localized at the moment of short-pulse photoexcitation.[26]

V. REMARKS ON BLOCH GAIN

Finally, we would like to mention that the phase of the transient current $\partial P(t)/\partial t$ is related to the spectral shape of the ac differential conductivity $\sigma(\omega)$ in the WS ladder regime, where the polarization increases linearly with the bias electric field. Since the Fourier transform of $\partial^2 P(t)/\partial t^2$ is calculated to be $-i\omega\chi(\omega)F$ from Eq. (5) and $\sigma(\omega)=-i\omega\chi(\omega)$ by definition, $\tilde{E}_{\mathrm{THz}}(\omega)$ is proportional to $\sigma(\omega)F$. Figure 7 shows Re $\tilde{E}_{\mathrm{THz}}(\omega)$ and Im $\tilde{E}_{\mathrm{THz}}(\omega)$ spectra obtained from the THz wave form of Fig. 4(a). As seen in the figure, Re $\tilde{E}_{\mathrm{THz}}(\omega)$ changes from negative to positive across $\omega_B/2\pi=2.0$ THz. Thus, the observed oscillation phase is consistent with the existence of inversionless gain below the Bloch frequency called the Bloch gain,[18,19,27] which appears as a quantum dissipative effect after the Bloch oscillation is dephased.[15,16,23]

Very recently, a few theoretical reports asserted that transient THz emission cannot be linked to the ac differential

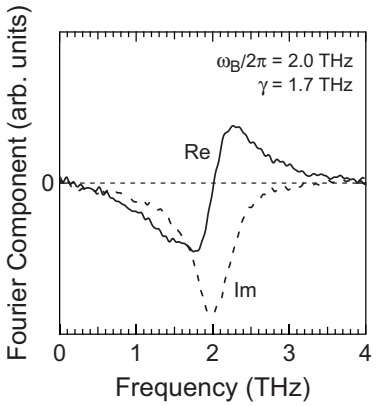

FIG. 7. Real and imaginary parts of the Fourier spectrum of the THz wave form shown in Fig. 4(a), where $\omega_B/2\pi=2.0$ THz and $\gamma=1.7$ THz.

conductivity in the WS ladder regime because the Esaki-Tsu nonlinear current-field relation does not allow linear-response analysis of the transient current for the optically switched step-function-like bias input.[22,28] However, they were based on the assumption that the transient current (or electron drift velocity) would start from zero at the moment of short-pulse photoexcitation, which is equal to its steady-state value for spatially extended electrons at $F=0$. Our experimental results with the time origin accurately determined by the MEM show that the transient current starts from its maximum as damped cos $\omega_B t$ for various pump photon energies E_{pm}, breaking the fundamental assumption of Refs. 22 and 28. We would like to emphasize that the observed transient current has a character of the polarization current created in a dielectric medium. It can indeed be identified as the polarization current under WS localization of electron wave functions, where the polarization approaches a linear asymptote with the bias electric field in the presence of the true current due to the hopping transport for the Esaki-Tsu dc conductivity.[25] Thus, the observed transient current is naturally linked to the steady-state ac dielectric property, i.e., the susceptibility $\chi(\omega)$, of WS-localized electrons for the optically switched step-function-like bias input.

This leads us to the conclusion that the ac differential conductivity $\sigma(\omega)=-i\omega\chi(\omega)$ can generally be measured from transient THz emission as long as electron transport occurs in a single energy band, i.e., the nonlinearity of the steady-state current-field relation arises only from the formation of a WS ladder.[14] It is not clear at present whether such a treatment is applicable to other types of THz gain ascribed to multiband electron transport.

VI. SUMMARY

In summary, we have systematically performed a phase-sensitive THz measurement of transient transport of Bloch oscillating electrons in the lowest miniband of GaAs-based SLs. The transient current has been found to always start from its maximum as damped cos $\omega_B t$ for various initial electron distributions created by femtosecond laser pulses. We have shown that the observed oscillation phase is governed by the translationally symmetric electron distribution under WS localization of electron wave functions, which cannot be equivalently described in the framework of semiclassical miniband transport before electrons experience Bragg reflections many times. Here, the transient current has been explained as the time derivative of the polarization that increases linearly with the bias electric field via the dielectric susceptibility $\chi(\omega)$ in the WS ladder regime. Thus, the observed oscillation phase is consistent with the spectral shape of the ac differential conductivity $\sigma(\omega)=-i\omega\chi(\omega)$ for the Bloch gain.

ACKNOWLEDGMENTS

We thank R. Ferreira, T. Ogawa, K. Asano, A. Shimizu, S. Komiyama, and H. Akiyama for stimulating discussions. This work was partly supported by Grants-in-Aid from JSPS (Grants No. 18201027 and No. 17-10614) and a Special Coordination Fund for Promoting Science and Technology from MEXT (NanoQuine). One of us (T.U.) is also grateful for financial support from JSPS.

*unuma@nuap.nagoya-u.ac.jp
†hirakawa@iis.u-tokyo.ac.jp

[1] F. Bloch, Z. Phys. **52**, 555 (1928).
[2] C. Zener, Proc. R. Soc. London, Ser. A **145**, 523 (1934).
[3] G. H. Wannier, Phys. Rev. **117**, 432 (1960).
[4] L. Esaki and R. Tsu, IBM J. Res. Dev. **14**, 61 (1970).
[5] S. A. Ktitorov, G. S. Simin, and V. Ya. Sindalovskii, Sov. Phys. Solid State **13**, 1872 (1972).
[6] E. E. Mendez, F. Agulló-Rueda, and J. M. Hong, Phys. Rev. Lett. **60**, 2426 (1988); P. Voisin, J. Bleuse, C. Bouche, S. Gaillard, C. Alibert, and A. Regreny, *ibid.* **61**, 1639 (1988).
[7] A. A. Ignatov, K. F. Renk, and E. P. Dodin, Phys. Rev. Lett. **70**, 1996 (1993).
[8] K. Unterrainer, B. J. Keay, M. C. Wanke, S. J. Allen, D. Leonard, G. Medeiros-Ribeiro, U. Bhattacharya, and M. J. W. Rodwell, Phys. Rev. Lett. **76**, 2973 (1996).
[9] A. A. Ignatov, E. P. Dodin, and V. I. Shashkin, Mod. Phys. Lett. B **5**, 1087 (1991).
[10] J. Feldmann, K. Leo, J. Shah, D. A. B. Miller, J. E. Cunningham, T. Meier, G. von Plessen, A. Schulze, P. Thomas, and S. Schmitt-Rink, Phys. Rev. B **46**, 7252 (1992); K. Leo, P. H. Bolivar, F. Brüggemann, R. Schwedler, and K. Köhler, Solid State Commun. **84**, 943 (1992).
[11] C. Waschke, H. G. Roskos, R. Schwedler, K. Leo, H. Kurz, and K. Köhler, Phys. Rev. Lett. **70**, 3319 (1993).
[12] A. M. Bouchard and M. Luban, Phys. Rev. B **52**, 5105 (1995).
[13] M. Helm, Semicond. Sci. Technol. **10**, 557 (1995).
[14] K. Leo, *High-Field Transport in Semiconductor Superlattices* (Springer, New York, 2003), pp. 1–33.
[15] A. Wacker, Phys. Rev. B **66**, 085326 (2002).

[16] H. Willenberg, G. H. Döhler, and J. Faist, Phys. Rev. B **67**, 085315 (2003).
[17] We obtained basically the same experimental results for samples with different structural parameters.
[18] Y. Shimada, K. Hirakawa, M. Odnoblioudov, and K. A. Chao, Phys. Rev. Lett. **90**, 046806 (2003).
[19] N. Sekine and K. Hirakawa, Phys. Rev. Lett. **94**, 057408 (2005).
[20] E. M. Vartiainen, Y. Ino, R. Shimano, M. Kuwata-Gonokami, Y. P. Svirko, and K.-E. Peiponen, J. Appl. Phys. **96**, 4171 (2004).
[21] L. Yang, B. Rosam, J.-M. Lachaine, K. Leo, and M. M. Dignam, Phys. Rev. B **69**, 165310 (2004).
[22] A. Lisauskas, M. M. Dignam, N. V. Demarina, E. Mohler, and H. G. Roskos, Appl. Phys. Lett. **93**, 021122 (2008).
[23] T. Unuma, N. Sekine, and K. Hirakawa, Appl. Phys. Lett. **89**, 161913 (2006).
[24] G. Bastard and R. Ferreira, C. R. Acad. Sci., Ser. II: Mec., Phys., Chim., Sci. Terre Univers **312**, 971 (1991).
[25] Each electron contributes to either P or J_{tr} with a probability governed by inter-WS-level scattering.
[26] The initial condition for fitting the observed THz wave form with a general oscillatory solution of the Boltzmann equation has been investigated by R. Ferreira, T. Unuma, K. Hirakawa, and G. Bastard, Appl. Phys. Express **2**, 062101 (2009). However, as described in the present paper, the semiclassical band picture itself gives no reasonable explanation for the choice of the obtained initial condition on the basis of electron distributions in momentum space.
[27] P. G. Savvidis, B. Kolasa, G. Lee, and S. J. Allen, Phys. Rev. Lett. **92**, 196802 (2004).
[28] P. Shiktorov, E. Starikov, V. Gružinskis, L. Varani, and L. Reggiani, Acta Phys. Pol. A **113**, 913 (2008).